materials proceedings

MDPI

Proceeding Paper

Influence of Electrospinning Parameters on the Physicochemical Properties of Polycaprolactone, Chitosan, and Sericin Membranes †

María Oviedo [1], Yuliet Montoya [1,*], Catalina Alvarez [2] and John Bustamante [1]

[1] Grupo de Dinámica Cardiovascular, Centro de Bioingeniería, Universidad Pontificia Bolivariana, Medellín 050031, Colombia; mariac.oviedo@upb.edu.co (M.O.); john.bustamante@upb.edu.co (J.B.)
[2] Grupo de Investigaciones Agroindustriales, Universidad Pontificia Bolivariana, Medellín 050031, Colombia; alvarezl.catalina@gmail.com
* Correspondence: yuliet.montoya@upb.edu.co
† Presented at the 7th International Conference on Advanced Polymer Materials and Nanocomposites, ANM 2023, Aveiro, Portugal, 26–28 July 2023.

Abstract: The use of natural polymers such as sericin (SS) and chitosan (Ch) for developing biomaterials has increased in tissue engineering. To ensure adequate biointegration with the biological environment, the method used to obtain the biomaterial plays an important role, which is why the electrospinning technique has been employed due to its versatility with regard to emulating the native extracellular matrix. The present study evaluated the influence of electrospinning parameters on the morphological, chemical, and thermal properties of polycaprolactone (PCL), Ch, and SS composite membranes. To achieve this, experiments were designed with varying manufacturing parameters and SS concentrations. The membranes were then characterized by scanning electron microscopy (SEM), Fourier transforms spectrophotometry (FTIR), and thermogravimetric analysis (TGA). SEM images showed that the electrospinning conditions and SS concentrations allow the development of electrospun membranes with high fibrillar density randomly oriented and fiber diameters below 100 nm. Likewise, the spectra and thermograms of the composite membranes show the possible chemical interactions and thermal behavior, demonstrating the homogeneity and stability of the fibrillar structure.

Keywords: chitosan; electrospinning; nanoarchitecture; sericin

Citation: Oviedo, M.; Montoya, Y.; Alvarez, C.; Bustamante, J. Influence of Electrospinning Parameters on the Physicochemical Properties of Polycaprolactone, Chitosan, and Sericin Membranes. *Mater. Proc.* **2022**, *11*, 5. https://doi.org/10.3390/materproc2022011005

Academic Editor: Elby Titus

Published: 27 October 2023

1. Introduction

Among the techniques used to manufacture biomaterials that emulate the native extracellular matrix is electrospinning, which allows the development of three-dimensional microarchitectures made up of micro and nanometer-sized fibrillar structures [1,2]. One of the main advantages of this technique is its ability to generate multilayers through the combination of parameters such as voltage, output flow, needle–collector distance, or relative humidity to obtain biomaterials that can exhibit biocompatible characteristics [3].

In addition, another versatility of electrospinning technique is that it allows the use of a wide variety of polymers of both natural and synthetic origin, making it possible to obtain fibrillar matrices with improved mechanical, absorption, biocompatibility, and biodegradability characteristics [4]. In this sense, sericin is a biocompatible and biodegradable protein obtained from Bombyx mori silkworm cocoons; it is mainly composed of polar groups such as hydroxyl, carboxyl, and amino [5,6]. Meanwhile, chitosan as a natural polymer has shown adequate biological, biodegradable, antibacterial, and wound-healing properties, which have made it a potential biomaterial of interest in the biomedical sector [7,8].

Based on the previous, and considering the advantages of the electrospinning technique for obtaining fibrillar matrices with morphological and biochemical characteristics dependent on the composition of the materials and the variation of the manufacturing parameters,

the present work was oriented to the development of electrospun membranes composed of polycaprolactone, medium molecular weight chitosan, and silk sericin to evaluate their morphological, chemical and thermal properties for their possible use as a biomaterial.

2. Experiments

2.1. Materials

Polycaprolactone (PCL) with a molecular weight of 80,000 Da and medium molecular weight chitosan (Ch) (190,000–310,000 Da) were purchased from Sigma Aldrich. Glacial acetic acid with 99.5% purity and formic acid with 99% purity was purchased from Merck Millipore. Sericin was extracted from cocoons that were supplied by Corporacion para el Desarrollo de la Sericultura del Cauca-CORSEDA (Cauca, Colombia).

2.2. Preparation of Material

2.2.1. Extraction of Sericin (SS)

The SS was extracted using a degumming technique at high temperature and pressure. To achieve this, the cocoons were cut into small pieces, and a bath ratio of 1:30 (g cocoon/mL of distilled water) was prepared. The mixture was transferred to an AV-75 Phoenix autoclave (Phoenix Luferco, Sao Paulo, Brazil) at a temperature of 120 °C for 30 min. The sericin solution was filtered to remove particulate matter present in the solution. Sericin powder was then obtained by spray drying.

2.2.2. Preparation of Work Solutions

Solutions of PCL at 12% w/V, Ch at 2% w/V, and SS at 1% w/V, 1.5% w/V, and 2% w/V were prepared using a mixture of formic and acetic acid as the solvent in 55:45 volumetric ratios. The resulting solutions were previously agitated for 24 hours, then the polymeric mixture of PCL/Ch, PCL/Ch/SS_1%, PCL/Ch/SS_1.5%, and PCL/Ch/SS_2% was made and agitated again for the same amount of time.

2.2.3. Preparation of Composite Membranes

PCL/Ch, PCL/Ch/SS_1%, PCL/Ch/SS_1.5%, and PCL/Ch/SS_2% blends were deposited in 5 mL glass syringes. The electrospinning conditions such as distance and flow rate were varied, while the voltage and volumetric ratio of the polymers remained fixed (see Table 1). All membranes were electrospun in a time of 8 h.

Table 1. Design of experiment for the development of PCL/Ch/SS electrospun membranes.

SS Concentration (% *w*/*w*)	Volumetric Ratio (*w*/*w*)	Parameters		
		Voltage (kV)	Flow (mL/h)	Needle-Collector Distance (cm)
0%	PCL: Ch (6:4)	22	0.25	20 25
			0.30	20 25
1%	PCL/Ch: SS (8:2)	22	0.25	20 25
			0.30	20 25
1.5%	PCL/Ch: SS (8:2)	22	0.25	20 25
			0.30	20 25
2%	PCL/Ch: SS (8:2)	22	0.25	20 25
			0.30	20 25

2.3. Characterization of the Material

2.3.1. Scanning Electron Microscopy (SEM)

The morphological characteristics were analyzed in a Jeol NeoScope JCM-600 (JEOL Ltd, Tokyo, Japan) plus scanning electron microscope at a power of 15 kV. Subsequently, to determine the average fiber diameter, the micrographs were analyzed at a magnification of 10,000× using ImageJ® software (National Institutes of Health and the Laboratory for Optical and Computational Instrumentation–University of Wisconsin, Madison, WI, USA). With the results obtained, the polydispersity index (PdI) of the fibers was calculated using (1).

$$\mathrm{PdI} = \left(\frac{\sigma}{\alpha}\right)^2 \quad (1)$$

where σ is the standard deviation of the fiber diameter distribution and α is the average fiber diameter [9].

2.3.2. Fourier Transform Spectroscopy (FTIR)

The chemical analysis of the functional groups was performed using Fourier transform spectrophotometry with a universal attenuated total reflection module (FTIR-UATR) using a Spectrum Two-PerkinElmer spectrophotometer (PerkinElmer, New York, NY, USA). The spectra were obtained at a resolution of 4 cm^{-1} from 4 scans performed at a wavelength between 400 and 4000 cm^{-1}.

2.3.3. Thermogravimetric Analysis (TGA)

TGA analysis of the membranes was carried out on a Mettler Toledo TGA/SDTA 851e (Mettler Toledo, Columbus, OH, USA). Thermograms were obtained in an inert N_2 atmosphere with a heating ramp of 10 °C/min in the temperature range of 25–800 °C.

2.3.4. Statistical Analysis

The results were analyzed using a factorial ANOVA study, where the statistical influence was determined through the assumption of p-value < α, which was corroborated using the Shapiro–Wilk normality test and Bartlett's homoscedasticity test, under the hypothesis of p-value > α. In addition, the values obtained in the characterization techniques are expressed as the mean ± standard deviation. Likewise, an n = 2 and a statistical significance level of $p < 0.05$ were considered for each method.

3. Results and Discussion

3.1. Scanning Electron Microscopy (SEM)

From the experimental design of the electrolytic conditions of PCL/CH composite solutions with different concentrations of SS, it was found that the parameters allowed us to obtain membranes with continuous, homogeneous, defect-free fibers and with fiber diameters distributed at the nanometer scale (see Figure 1).

From the results obtained, it was evident that the inclusion of different volumetric ratios of SS in PCL/Ch membranes does not generate differences in the deposition, orientation, and fiber diameter of electrospun membranes, indicating that sericin does not affect the viscosity and conductivity of the solution [10]. Likewise, no correlation behavior of parameters such as distance and flow on the fiber diameter was observed. This might be associated with the fact that the reported ranges of these parameters in conjunction with the voltage value confer similar stability in the Taylor cone, causing the formation of fibers with diameters between 50 and 100 nm (see Table 2) [11]. This result could also be attributed to the polycationic nature of the chitosan and the sericin charges that confer stability in conductivity due to the charge density, which in turn allows an elongation of the fiber and a decrease in diameter [12,13].

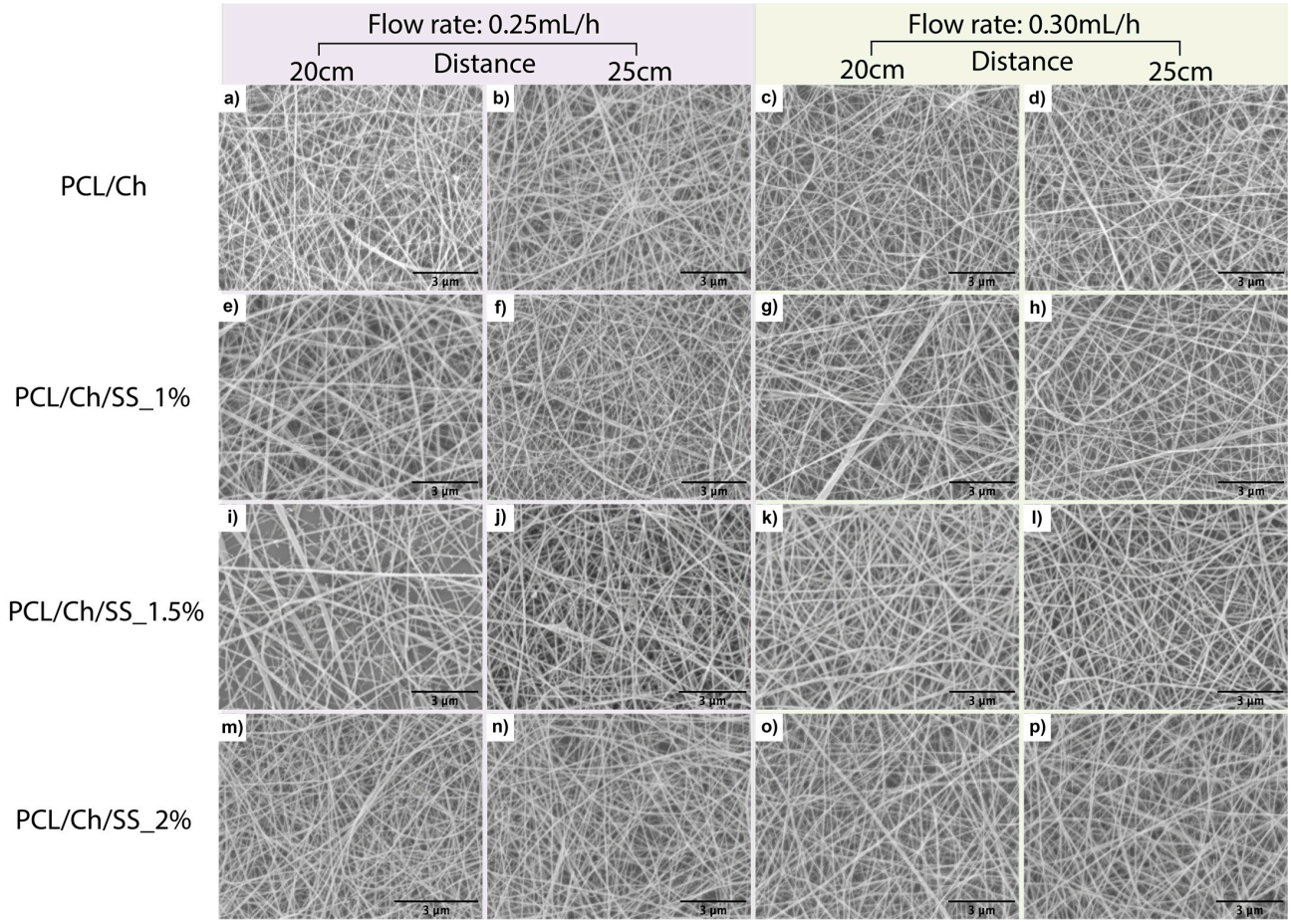

Figure 1. Micrographs of electrospun membranes with parameters; PCL/Ch (**a**) 20 cm; 0.25 mL/h, (**b**) 25 cm; 0.25 mL/h, (**c**) 20 cm; 0.30 mL/h, (**d**) 25 cm; 0.30 mL/h; PCL/Ch/SS_1% (**e**) 20 cm y 0.25 mL/h, (**f**) 25 cm y 0.25 mL/h, (**g**) 20 cm y 0.30 mL/h, (**h**) 25 cm y 0.30 mL/h; PCL/Ch/SS_1.5% (**i**) 20 cm y 0.25 mL/h, (**j**) 25 cm y 0.25 mL/h, (**k**) 20 cm y 0.30 mL/h, (**l**) 25 cm y 0.30 mL/h; PCL/Ch/SS_2% (**m**) 20 cm y 0.25 mL/h, (**n**) 25 cm y 0.25 mL/h, (**o**) 20 cm y 0.30 mL/h, (**p**) 25 cm y 0.30 mL/h.

Table 2. Fiber diameter and PdI of biocomposite electrospun membranes.

Type of Material	Electrospinning Parameters	Fiber Diameter	PdI
PCL/Ch	0.25 mL/h; 20 cm	66 ± 8	0.014
	0.25 mL/h; 25 cm	73 ± 13	0.034
	0.30 mL/h; 20 cm	77 ± 2	0.001
	0.30 mL/h; 25 cm	75 ± 2	0.001
PCL/Ch/SS_1%	0.25 mL/h; 20 cm	88 ± 13	0.021
	0.25 mL/h; 25 cm	78 ± 9	0.014
	0.30 mL/h; 20 cm	59 ± 12	0.042
	0.30 mL/h; 25 cm	82 ± 7	0.007
PCL/Ch/SS_1.5%	0.25 mL/h; 20 cm	97 ± 30	0.094
	0.25 mL/h; 25 cm	82 ± 8	0.011
	0.30 mL/h; 20 cm	91 ± 8	0.009
	0.30 mL/h; 25 cm	87 ± 8	0.010
PCL/Ch/SS_2%	0.25 mL/h; 20 cm	77 ± 2	0.001
	0.25 mL/h; 25 cm	82 ± 1	0.000
	0.30 mL/h; 20 cm	91 ± 1	0.000
	0.30 mL/h; 25 cm	79 ± 7	0.008

On the other hand, it was determined that PCL/Ch, PCL/Ch/SS_1%, PCL/Ch/SS_1.5%, and PCL/Ch/SS_2% membranes presented polydispersity indices lower than 0.1, indicating that the fiber diameters exhibit monodisperse behavior (see Table 2).

3.2. Fourier Transform Spectroscopy (FTIR)

The spectra in Figure 2 show the characteristic spectral bands of the functional groups present in the membranes PCL/Ch, PCL/Ch/SS_1%, PCL/Ch/SS_1.5%, and PCL/Ch/SS_2%. Figure 2a shows the presence of two spectral bands of PCL located at wavelengths between 2940 and 2944 cm^{-1} and 1724–1726 cm^{-1}, corresponding to the vibration of the -CH and -C=O groups [14]. In addition, we identified characteristic peaks in the Ch spectrum, such as the band between 3000 and 3500 cm^{-1} associated with the vibration of the -OH groups and primary amines, the band at a wavelength between 2867 and 2870 cm^{-1}, related to the stretching of the -CH bond, and a spectral region between 1700 and 1000 cm^{-1} where the absorption bands for amide I (1670–1690 cm^{-1}) and amide II (1580 and 1586 cm^{-1}) are observed. Finally, the vibration of the groups -CH3 at wavelengths of 1366 cm^{-1} and -CO at a length of 1048 cm^{-1} was found [15,16].

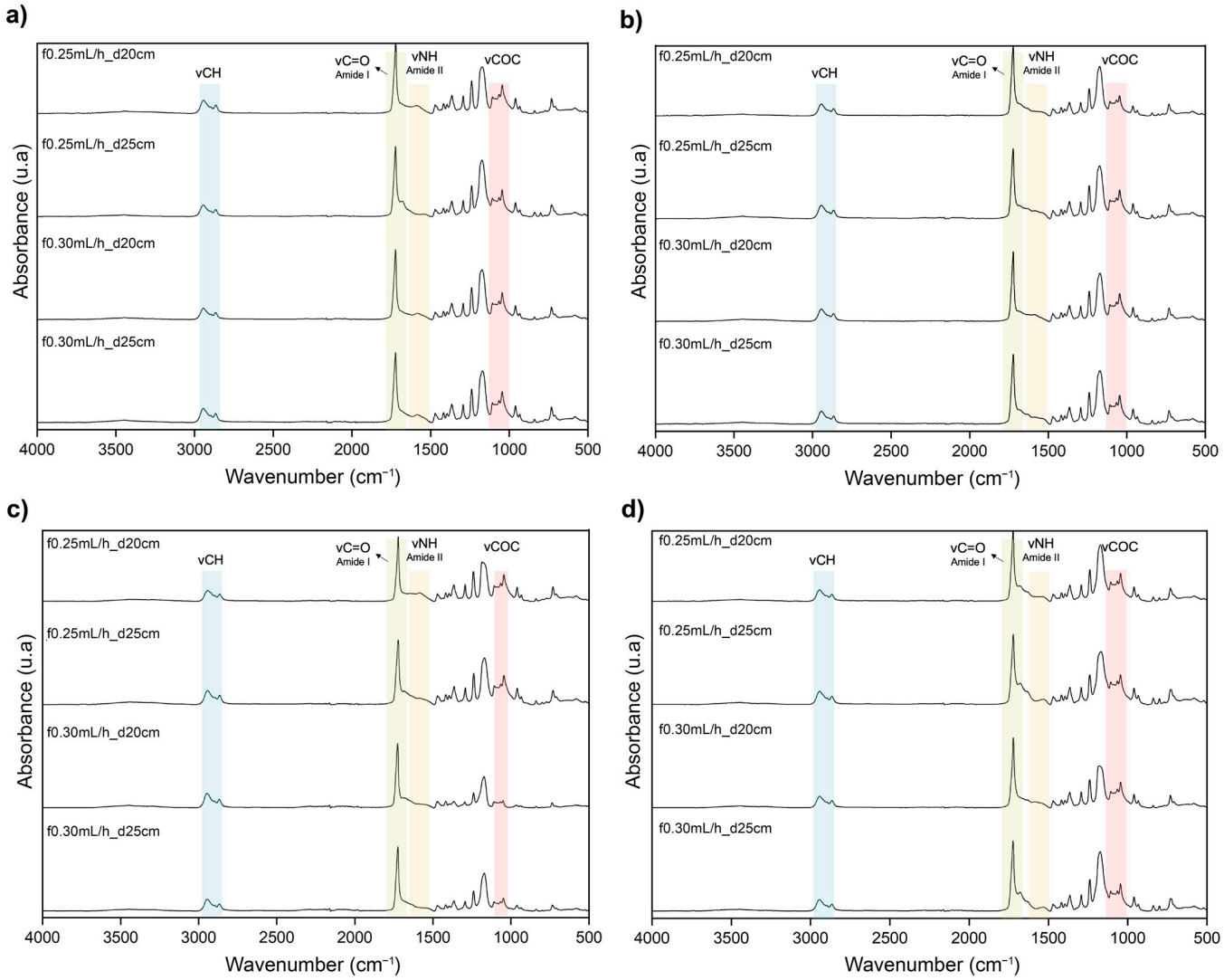

Figure 2. FTIR spectra of electrospun membranes (**a**) PCL/Ch, (**b**) PCL/Ch/SS_1%, (**c**) PCL/Ch/SS_1.5% and (**d**) PCL/Ch/SS_2%.

On the other hand, in Figure 2b–d, the characteristic absorption bands of sericin were evidenced, where amide I (1670–1690 cm^{-1}), amide II (1552–1570 cm^{-1}) and amide III

(1240–1250 cm^{-1}) are found. These bands correspond with the stretching C=O, N-H and C-N, which coincides with the characteristic peaks of a random coil structure. Similarly, the presence of the C-H and O-H bending vibrations in the band of 1390–1394 cm^{-1} and the C-OH stretching vibration between 1064 and 1070 cm^{-1} is denoted [17–19].

Finally, a displacement of the band corresponding to amide II of the electrospun membranes composed of PCL/Ch/SS of the different concentrations was evidenced, presenting wavelengths between 1552–1570 cm^{-1} compared to the PCL/Ch controls, which were located between 1580 and 1586 cm^{-1}. Such behavior could be attributed to an interaction mediated by weak bonds between the carbonyl and amino groups of SS and the hydroxyl or amine groups of chitosan, indicating that SS is integrated into the PCL/Ch structure [15].

3.3. Thermogravimetric Analysis (TGA)

Figure 3 shows the thermograms that allow the identification of the degradation and thermal stability of the PCL/Ch and PCL/Ch/SS composite samples at different sericin concentrations and electrospinning parameters. The weight loss of PCL/Ch membranes starts with a percentage of 2% to 3% between 97 and 100 °C, which may be associated with the evaporation of water molecules in the sample or the mixture of solvents, since both present their boiling point approximately 100–120 °C. Next, a weight loss of up to 18% was observed between 238 and 244 °C, which could be associated with the beginning of chitosan degradation due to the presence of a free amino group in its structure, and finally, a continuous weight loss was observed between 350 and 450 °C, which was associated with the degradation of the polycaprolactone and chitosan until a final loss percentage of 90–95% was obtained (see Figure 3a) [20,21].

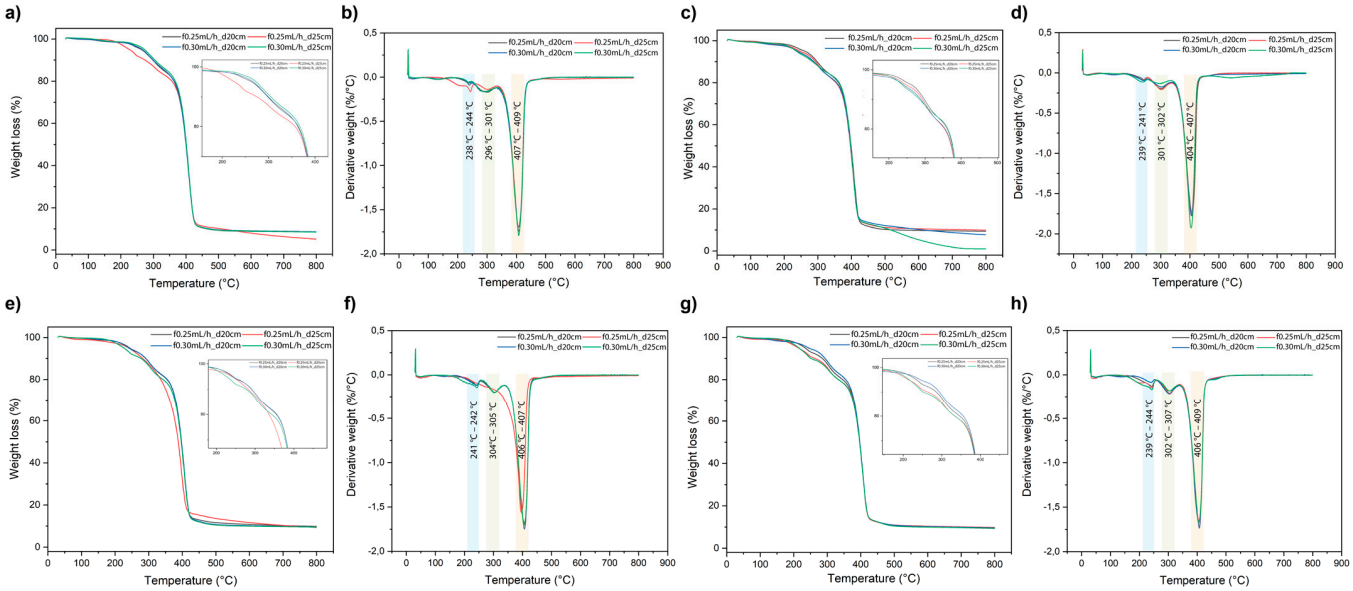

Figure 3. Thermograms of TGA and derivate thermogravimetry (DTG) of membranes (**a**) TGA of PCL/Ch, (**b**) DTG of PCL/Ch, (**c**) TGA of PCL/Ch/SS_1%, (**d**) DTG of PCL/Ch/SS_1% (**e**) TGA of PCL/Ch/SS_1.5%, (**f**) DTG of PCL/Ch/SS_1.5%, (**g**) TGA of PCL/Ch/SS_2% and (**h**) DTG of PCL/Ch/SS_2%.

Similarly, the PCL/Ch composite samples with different SS concentrations show similar behavior to the degradation of the PCL/Ch samples. Between 96 and 100 °C, moisture vaporization and solvent mixing occur; between 200 and 350 °C, the mass loss tendency is 15–18% due to the degradation of the amino group of chitosan and the peptide and amino acid bonds of SS, since the amorphous structures of this protein begin their degradation around 210 °C; and finally, between 350 and 425 °C, there is a continuous degradation of PCL, Ch, and SS obtaining a final mass percentage of 90–95%. On the other hand, all the samples composed of PCL/Ch/SS and the PCL/Ch controls show three

degradation peaks located between 239 and 242 °C; 301 and 305 °C; and 404 and 407 °C, which indicates that the thermal degradation behavior is not affected by the changes generated in the microarchitecture of the membranes as a result of the changes in the electrospinning parameters [17,22].

4. Conclusions

In this study, it was possible to obtain a range of electrospinning conditions and SS concentrations that allow the development of homogeneous electrospun membranes, with high fibrillar density randomly oriented and fiber diameters below 100 nm. Additionally, it was found that incorporating SS in PCL/Ch membranes maintains the polycationic charge density of the chitosan, which favors the conductivity of the solution that influences the stability of the electrospinning. On the other hand, the spectra and thermograms of the composite membranes show the possible chemical interactions and the thermal decomposition behavior, demonstrating the homogeneity and stability of the fibrillar structure.

Author Contributions: Conceptualization, Y.M. and J.B.; methodology, M.O., C.A., Y.M. and J.B.; software, M.O. and Y.M.; validation, M.O., Y.M. and C.A.; formal analysis, M.O. and Y.M.; investigation, M.O., Y.M., C.A. and J.B.; resources, Y.M., C.A. and J.B.; data curation, M.O., C.A. and Y.M.; writing—original draft preparation, M.O., Y.M., C.A. and J.B.; writing—review and editing, M.O., Y.M., C.A. and J.B.; visualization, M.O. and Y.M.; supervision, Y.M., C.A. and J.B.; project administration, C.A., Y.M. and J.B.; funding acquisition, C.A., Y.M. and J.B. All authors have read and agreed to the published version of the manuscript.

Funding: Thanks to the Ministerio de Ciencia, Tecnología e Innovación MINCIENCIAS, Colombia, for the support with the project 121084468254. Additionally, we wish to thank the Sistema General de Regalías SGR, Colombia for the funding with the project 2020000100190.

Institutional Review Board Statement: Not applicable.

Informed Consent Statement: Not applicable.

Data Availability Statement: Not applicable.

Conflicts of Interest: The authors declare no conflict of interest.

References

1. Mochane, M.J.; Motsoeneng, T.S.; Sadiku, E.R.; Mokhena, T.C.; Sefadi, J.S. Morphology and Properties of Electrospun PCL and Its Composites for Medical Applications: A Mini Review. *Appl. Sci.* **2019**, *9*, 2205. [CrossRef]
2. Ghaee, A.; Bagheri-Khoulenjani, S.; Amir Afshar, H.; Bogheiri, H. Biomimetic Nanocomposite Scaffolds Based on Surface Modified PCL-Nanofibers Containing Curcumin Embedded in Chitosan/Gelatin for Skin Regeneration. *Compos. B Eng.* **2019**, *177*, 107339. [CrossRef]
3. Erickson, A.E.; Edmondson, D.; Chang, F.C.; Wood, D.; Gong, A.; Levengood, S.L.; Zhang, M. High-throughput and high-yield fabrication of uniaxially-aligned chitosan-based nanofibers by centrifugal electrospinning. *Carbohydr. Polym.* **2015**, *134*, 467–474. [CrossRef]
4. Nagam Hanumantharao, S.; Rao, S. Multi-Functional Electrospun Nanofibers from Polymer Blends for Scaffold Tissue Engineering. *Fibers* **2019**, *7*, 66. [CrossRef]
5. Vineis, C.; Cruz Maya, I.; Mowafi, S.; Varesano, A.; Sánchez Ramírez, D.O.; Abou Taleb, M.; Tonetti, C.; Guarino, V.; El-Sayed, H. Synergistic Effect of Sericin and Keratin in Gelatin Based Nanofibers for in Vitro Applications. *Int. J. Biol. Macromol.* **2021**, *190*, 375–381. [CrossRef]
6. Li, L.; Qian, Y.; Lin, C.; Li, H.; Jiang, C.; Lv, Y.; Liu, W.; Cai, K.; Germershaus, O.; Yang, L. The Effect of Silk Gland Sericin Protein Incorporation into Electrospun Polycaprolactone Nanofibers on in Vitro and in Vivo Characteristics. *J. Mater. Chem. B* **2015**, *3*, 859–870. [CrossRef]
7. Machado, B.R.; Roberto, S.B.; Bonafé, E.G.; Camargo, S.E.A.; Camargo, C.H.R.; Popat, K.C.; Kipper, M.J.; Martins, A.F. Chitosan Imparts Better Biological Properties for Poly(ε-Caprolactone) Electrospun Membranes than Dexamethasone. *J. Braz. Chem. Soc.* **2019**, *30*, 1741–1750. [CrossRef]
8. Chameettachal, S.; Murab, S.; Vaid, R.; Midha, S.; Ghosh, S. Effect of Visco-Elastic Silk–Chitosan Microcomposite Scaffolds on Matrix Deposition and Biomechanical Functionality for Cartilage Tissue Engineering. *J. Tissue Eng. Regen. Med.* **2017**, *11*, 1212–1229. [CrossRef]
9. Clayton, K.N.; Salameh, J.W.; Wereley, S.T.; Kinzer-Ursem, T.L. Physical Characterization of Nanoparticle Size and Surface Modification Using Particle Scattering Diffusometry. *Biomicrofluidics* **2016**, *10*, 054107. [CrossRef] [PubMed]

10. Chanda, A.; Adhikari, J.; Ghosh, A.; Chowdhury, S.R.; Thomas, S.; Datta, P.; Saha, P. Electrospun Chitosan/Polycaprolactone-Hyaluronic Acid Bilayered Scaffold for Potential Wound Healing Applications. *Int. J. Biol. Macromol.* **2018**, *116*, 774–785. [CrossRef] [PubMed]
11. Zhao, R.; Li, X.; Sun, B.; Tong, Y.; Jiang, Z.; Wang, C. Nitrofurazone-Loaded Electrospun PLLA/Sericin-Based Dual-Layer Fiber Mats for Wound Dressing Applications. *RSC Adv.* **2015**, *5*, 16940–16949. [CrossRef]
12. Zhao, R.; Li, X.; Sun, B.; Zhang, Y.; Zhang, D.; Tang, Z.; Chen, X.; Wang, C. Electrospun Chitosan/Sericin Composite Nanofibers with Antibacterial Property as Potential Wound Dressings. *Int. J. Biol. Macromol.* **2014**, *68*, 92–97. [CrossRef] [PubMed]
13. Hadipour-Goudarzi, E.; Montazer, M.; Latifi, M.; Aghaji, A.A.G. Electrospinning of Chitosan/Sericin/PVA Nanofibers Incorporated with in Situ Synthesis of Nano Silver. *Carbohydr. Polym.* **2014**, *113*, 231–239. [CrossRef] [PubMed]
14. Sowmya, B.; Panda, P.K. Electrospinning of Poly(ε-Caprolactone) (PCL) and Poly Ethylene Glycol (PEG) Composite Nanofiber Membranes Using Methyl Ethyl Ketone (MEK) and N N′-Dimethyl Acetamide (DMAc) Solvent Mixture for Anti-Adhesion Applications. *Mater. Today Commun.* **2022**, *33*, 104718. [CrossRef]
15. Karahaliloglu, Z.; Kilicay, E.; Denkbas, E.B. Antibacterial Chitosan/Silk Sericin 3D Porous Scaffolds as a Wound Dressing Material. *Artif. Cells Nanomed. Biotechnol.* **2017**, *45*, 1172–1185. [CrossRef] [PubMed]
16. Verma, J.; Kanoujia, J.; Parashar, P.; Tripathi, C.B.; Saraf, S.A. Wound Healing Applications of Sericin/Chitosan-Capped Silver Nanoparticles Incorporated Hydrogel. *Drug Deliv. Transl. Res.* **2017**, *7*, 77–88. [CrossRef] [PubMed]
17. Jena, K.; Pandey, J.P.; Kumari, R.; Sinha, A.K.; Gupta, V.P.; Singh, G.P. Free Radical Scavenging Potential of Sericin Obtained from Various Ecoraces of Tasar Cocoons and Its Cosmeceuticals Implication. *Int. J. Biol. Macromol.* **2018**, *120*, 255–262. [CrossRef] [PubMed]
18. Jo, Y.N.; Um, I.C. Effects of Solvent on the Solution Properties, Structural Characteristics and Properties of Silk Sericin. *Int. J. Biol. Macromol.* **2015**, *78*, 287–295. [CrossRef] [PubMed]
19. Ekasurya, W.; Sebastian, J.; Puspitasari, D.; Asri, P.P.P.; Asri, L.A.T.W. Synthesis and Degradation Properties of Sericin/PVA Hydrogels. *Gels* **2023**, *9*, 76. [CrossRef]
20. Herrera-Kao, W.A.; Loría-Bastarrachea, M.I.; Pérez-Padilla, Y.; Cauich-Rodríguez, J.V.; Vázquez-Torres, H.; Cervantes-Uc, J.M. Thermal Degradation of Poly(Caprolactone), Poly(Lactic Acid), and Poly(Hydroxybutyrate) Studied by TGA/FTIR and Other Analytical Techniques. *Polym. Bull.* **2018**, *75*, 4191–4205. [CrossRef]
21. Wang, F.; Liu, K.; Xi, Y.; Li, Z. One-Step Electrospinning PCL/Ph-LPSQ Nanofibrous Membrane with Excellent Self-Cleaning and Oil-Water Separation Performance. *Polymer* **2022**, *249*, 124858. [CrossRef]
22. Castrillón Martínez, D.C.; Zuluaga, C.L.; Restrepo-Osorio, A.; Álvarez-López, C. Characterization of Sericin Obtained from Cocoons and Silk Yarns. *Procedia Eng.* **2017**, *200*, 377–383. [CrossRef]